Application of a Combined Model of Sediment Production, Supply and Runoff

Kazuki YAMANOI[1,*] and Masaharu FUJITA[2]

[1] Graduate School of Engineering, Kyoto University (Kyoto daigaku-katsura, Nishikyo-ku, Kyoto, 615-8530, JAPAN)

[2] Disaster Prevention Research Institute, Kyoto University (Gokasyo, Uji, Kyoto 6110011, Japan)

*Corresponding author. E-mail: yamanoi.kazuki.57n@st.kyoto-u.ac.jp

Sediment runoff process consists of three sub-processes: sediment production, supply, and transport. Although several numerical simulation models of sediment runoff have been proposed in relation to sediment management, they rely on empirical or statistical methods to generate the calculation conditions, which make it difficult to apply in a wide range of meteorological conditions. Similarly, sediment runoff processes are difficult to trace in detail using these models, and the numerical model is only able to output limited results as it is designed mainly to focus on sediment movement in rivers. To solve such problems, a new sediment runoff model has been developed that integrates various sub-processes used in numerical models. In this paper, the integrated model was applied to an actual, small mountainous watershed and analyzed in relation to the sediment runoff process on an annual scale. As a result of application, the change in volume of deposited sediment as taluses, and on the riverbed, was calculated and spatially visualized using GIS processing. In addition, the mean diameter change of the bed material in each unit channel was calculated. Results showed differences between the characteristics of each channel, which can be attributed to differences in the distance between each channel and the sediment source. Additionally, the relationship between water discharge and sediment discharge is discussed with reference to the location and timing of sediment supply. Results indicate that the positional relationship between the sediment source and a channel strongly influences the sediment runoff process. It is considered that this integrated model can provide detailed information for use in sediment management.

Key words: sediment production, sediment supply, sediment transport, freeze-thaw action

1. INTRODUCTION

To aid sediment management planning in rivers (particularly after huge sediment disasters), several numerical calculation models for sediment runoff have been previously proposed [*Sunada* and *Hasegawa*, 1994; *Egashira* and *Matsuki*, 2000; *Takahashi et al.*, 2000; *Murakami et al.*, 2001; *Mouri et al.*, 2003]. However, these models have been difficult to apply in a wide range of meteorological conditions because they rely on certain statistical or empirical methods to generate calculation conditions. In addition, the numerical model is only able to output limited results to enable synthetic sediment management, because the model is designed to mainly focus on the movement of sediment in rivers. It is also note that when using these models it is difficult to obtain results relating to important information within a mountainous watershed, such as the deposited sediment around a channel and the fresh sediment produced on a mountain slope. With such evident limitations, it is difficult to trace the entire sediment runoff process using these models.

However, to ameliorate such issues pertaining to past models, we have developed a new sediment runoff model [*Yamanoi* and *Fujita*, 2014; *Fujita et al.,* 2014]. **Fig. 1** shows a picture of typical phenomena that are targets of the model. The sediment runoff process is perceived here as a combination of three sub-processes: sediment production, sediment supply, and sediment transport. Sediment production is defined as a process whereby fresh soil is produced by an external agency (i.e. via freeze-thaw action, landslide, or volcanic eruption). Our studies mainly use models of freeze-thaw action as proposed by *Izumiyama et al.* [2012]. Following sediment production, the sediment generally drops to the bottom of a valley where it forms a talus, which is eroded during times

of flooding, and in our calculation model, this process is defined as the sediment supply sub-process. The sediment then flows downstream within the river, defined as sediment transport.

We applied the integrated model to an actual, small watershed in Takayama city, Gifu Prefecture, Japan, and we discuss here the rate of sediment production and riverbed evolution occurring in different areas within the watershed [*Fujita et al.,* 2014]. In addition, the seasonal variation in the relationship between sediment discharge and water discharge (at the observation station near the outlet of the basin) is discussed in the study.

We consider that the best feature our model offers is its ability to trace the process of sediment runoff both spatially and temporally, which has not previously been discussed in detail in other studies. The objective of this paper, therefore, is to examine the performance of this model and to verify its advantages by applying it to an actual watershed. Therefore, the complete sediment runoff process is discussed in detail. Firstly, the temporal variations in sediment deposition volume in the form of taluses, and on the river bed, are visualized spatially. Secondly, changes in the mean diameter of the river bed material at different points are discussed, and finally, the relationship between sediment discharge and water discharge at different points is compared, focusing on sediment supply and transport.

2. GENERAL DESCRIPTION OF THE INTEGRATED MODEL

In this chapter, we introduce a general description of the integrated sediment runoff model that we previously developed [*Yamanoi* and *Fujita,* 2014; *Fujita et al.,* 2014]. The model was developed by integrating sub-process models of sediment production, sediment supply, and sediment transport using a basin model composed of unit channels and unit slopes.

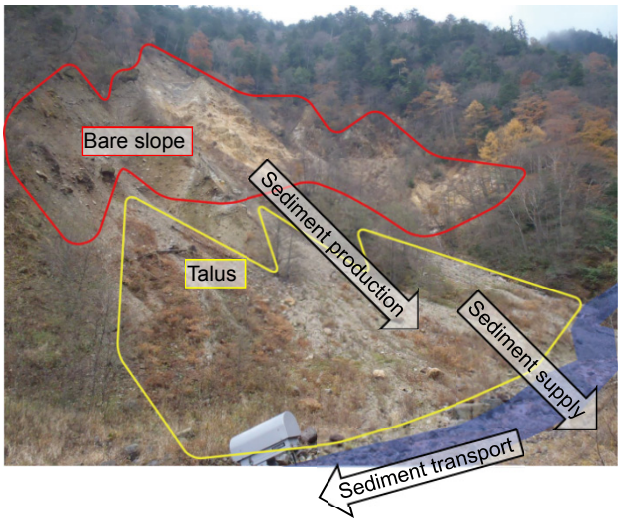

Fig. 1 Schematic picture of the target process

2.1 Basin model

The unit channels and unit slopes were extracted by GIS processing using the script of GRASS-GIS. The unit slopes were described by their rectangular inclined planes, and unit channels were assumed to be straight lines between two adjacent confluence points. **Fig. 2** shows a conceptual sketch of this model. The upstream boundary was set at a point where the catchment area measured 125,000 m^2. The length of the each unit channel was extracted automatically using GIS, and the inclination of the unit channel was calculated by dividing the difference in the elevation between the upstream end and the downstream end by the length of the channel. The area of each unit slope was then calculated using GIS by measuring the projected area of each slope, and the angle was calculated as the average angle on the actual slope. The channels are located in the center of the valleys, and the width of these valleys, B_{vi}, which is considered to be an important factor within the sediment supply model was extracted using the following equation:

$$B_{vi} = \frac{A_{vi}}{l_i} \tag{1}$$

where l_i = the length of the channel, and A_{vi} is the area of the valley, which can be calculated by extracting the area where the height difference from the channel is less than a particular value, assumed to be 1m in this paper in relation to the resolution of DEM data.

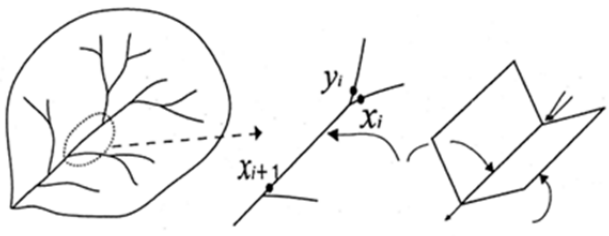

Fig. 2 Conceptual sketch of unit channels and unit slopes [after *Egashira* and *Matsuki* 2000]

2.2 Sub-process models

2.2.1 Sediment production model

Although several studies on sediment production have been conducted in the context of fields such as geology, hydrology, and hydraulics [*Matsuoka*, 1990; *Wegmann et al.,* 1998; *Fujita et al.,* 2005; *Tsutsumi et al.,* 2007], the numerical calculation method (which can estimate both the amount and timing of sediment production) has not actually been verified in practical use.

We have therefore developed a sediment production model based on *Izumiyama* [2012] and *Tsutsumi et al*. [2007]. Our model can calculate the vertical distribution of temperature under the bare slope surface and estimate the sediment production rate in relation to freeze-thaw action in several geological features categorized as either soft bedrock (i.e., weathered granite, weathered granite porphyry, and weathered shale) or hard bedrock (i.e., weathered sandstone and weathered rhyolite). For areas of pyroclastic flow deposits, we employed an equation that can estimate the annual erosion depth of the bare slope from the height of the bare slope [*Ashida et al*., 1983].

2.2.2 Sediment supply model

Our sediment supply model was developed in relation to talus erosion. This model calculates the erosion rate of a talus in consideration of the stream width which is estimated using water discharge, and valley width as extracted by GIS processing [*Fujita et al.,* 2014]. The timing involved in sediment supply and the change of the sediment storage volume of a talus were expressed by these models. The talus is eroded when the channel width increases, according to a rise of water level and arrives at the toe of talus. The inclination of the bedrocks and the surface of the talus are assumed to be constantly 50 degrees and 35 degrees. The basic equation used is describes below:

$$B_{ci} = \alpha\sqrt{Q_i} \tag{2}$$

$$S_{gi}(t) = \frac{1}{l_{ti}}\left(\int_0^t Q_{proi}(t)dt - \int_0^t Q_{supi}(t)dt\right) + S_{gi0} \tag{3}$$

$$Q_{supi}(t) = \begin{cases} l_{ti}H_{si}(t)\dfrac{dL}{dt} & when \quad L > 0 \\ 0 & when \quad L \le 0 \end{cases} \tag{4}$$

$$L = B_{si}(t) + B_{ci}(t) - B_{vi} \tag{5}$$

where B_{ci} = the stream width in unit channel *i;* α = a coefficient (assumed as 3.5 in the target watershed) [*Sawada et al.,* 1982]; Q_i = the water discharge in the unit channel *i*; S_{gi} = the talus volume per unit length; l_{ti} = the length of the talus equal to the bare slope width; $Q_{proi}(t)$ = the amount of sediment production per unit time, estimated by the sediment production model; $Q_{supi}(t)$ = the amount of sediment supply to the stream per unit time; S_{gi0} = the initial talus volume per unit length; $H_{si}(t)$ is the height of the talus; L is the function of length; $B_{si}(t)$ = the width of the talus. Each parameter for the length of a talus is described in **Fig.3**.

2.2.3 Sediment transport model

We employed the existing sediment transport model proposed by *Egashira* and *Matsuki* [2000]. The riverbed elevation and grain size distribution in each unit channel were calculated using this model. The grain size distribution of riverbed material was considered in the exchange layer, transition layer, and deposited layers [*Liu*, 1991], and the rainfall runoff was simulated simultaneously using the kinematic wave method and Darcy's law. The supplied sediment was expressed as riverbed evolution at the nearest unit channel.

2.3 Integration of three models

The GRASS-GIS was employed not only to extract basic topographical data but also to exchange output data between each numerical model. As a result of the integration, water and sediment discharge, volume of talus deposition, riverbed elevation, and grain size distribution were calculated for each unit channel from meteorological data, DEM (Digital Elevation Model) data, bare slope data, and the initial grain size distribution.

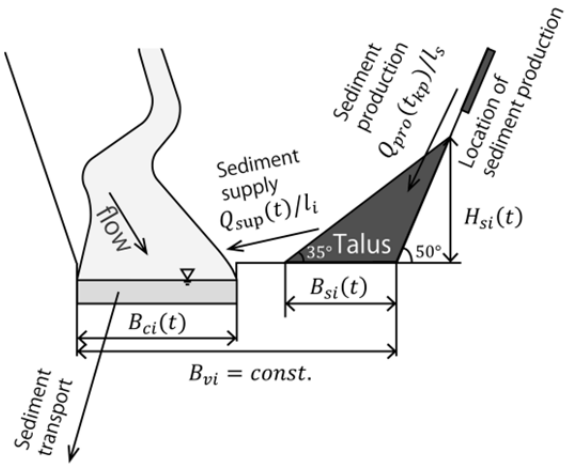

Fig. 3 Concept of the talus erosion model [after *Fujita et al.* 2014]

3. APPLICATION OF THE INTEGRATED MODEL

3.1 Condition of calculation

The integrated model was applied to the target watershed (**Fig. 4** shows a map of the area). The area of the watershed is around 7 km^2 and elevation of this watershed is distributed from 1000m to 2350m. The average river bed slope is 16.5 degrees. The mean annual precipitation was 1965.5 mm (1981~2010) at the nearest rainfall gage of Japan Meteorological Agency. We classified the geological features into 3 categories; soft rock, hard rock, and pyroclastic flow deposits. The characteristics of the sediment production due to freeze thaw action on the serpentinite bed rocks is not clear because the experiment of freeze thaw action on the serpentinite rocks is not conducted yet. We therefore assumed that it is classified into hard rock group considering the general lithological characteristics of serpentinite. The channels were extracted from 5 m mesh DEM data published by the Geospatial Information Authority of Japan. For the calculation of sediment production, we employed meteorological data (e.g., air temperature, solar radiation, wind velocity, and humidity) from 2011 to 2012 observed at a station near point A. The average air temperature here was 7.1 ℃ in 2006~2012. The lapse-rate of air temperature is set for 0.6 [℃/100m] to consider the altitudinal distribution of it. For the sediment supply and transport calculation, we used the rainfall data from April–November 2012, as observed by a C-band radar system to consider the spatial distribution of rainfall intensity.

The grain size distribution of the produced sediment and river bed material were considered to be very important parameters for use in this sediment runoff model. We therefore observed the grain-size distribution of produced sediment deposited as taluses in the area of each geological feature (e.g., soft rock, pyroclastic flow deposits, and hard rock), and the results are shown in **Fig. 5** (the grain-size distribution of riverbed material at a representative point is also shown in **Fig. 5**). However, it was considered that the grain-size distribution of riverbed materials differs widely depending on the location of the channel. We therefore conducted a five-year pre-calculation using the grain size distribution data (Fig.5) and rainfall data from 2007 to 2011 at a gauge station located near the basin **Fig. 6** shows the results of this pre-calculation of the mean diameter of exchange layer in each unit channel, and shows that the mean grain size of riverbed sediment was relatively reduced in the downstream channels or near to bare-slopes.

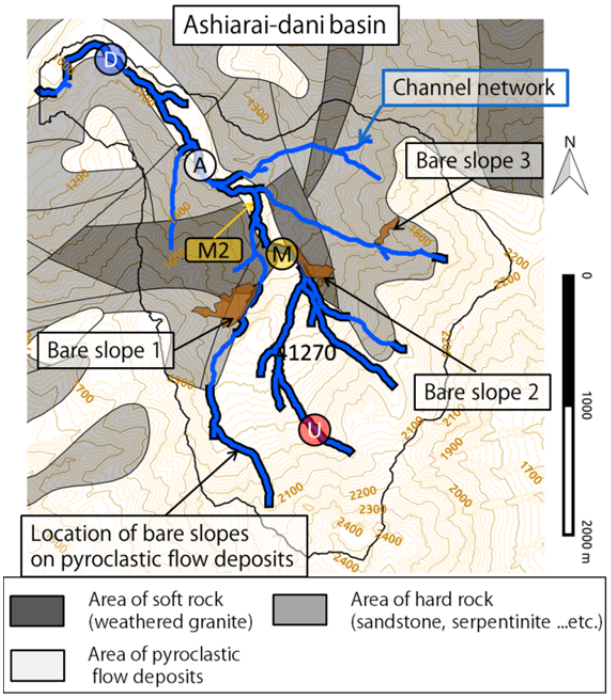

Fig. 4 Unit channels, categorized geological features, and sediment sources in the watershed. Locations used for calculation results are denoted by circles

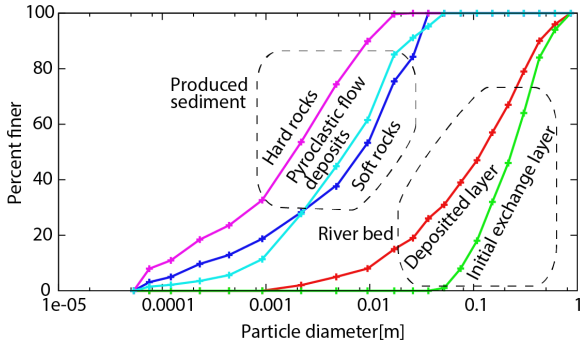

Fig. 5 Grain size distribution in each geological feature (using same conditions as [*Fujita et al.*, 2014])

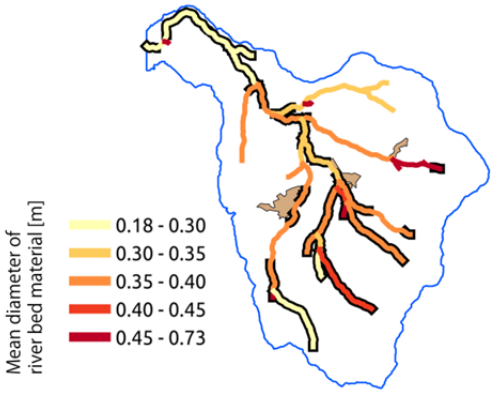

Fig. 6 Mean diameter of exchange layer in riverbed material in each channel

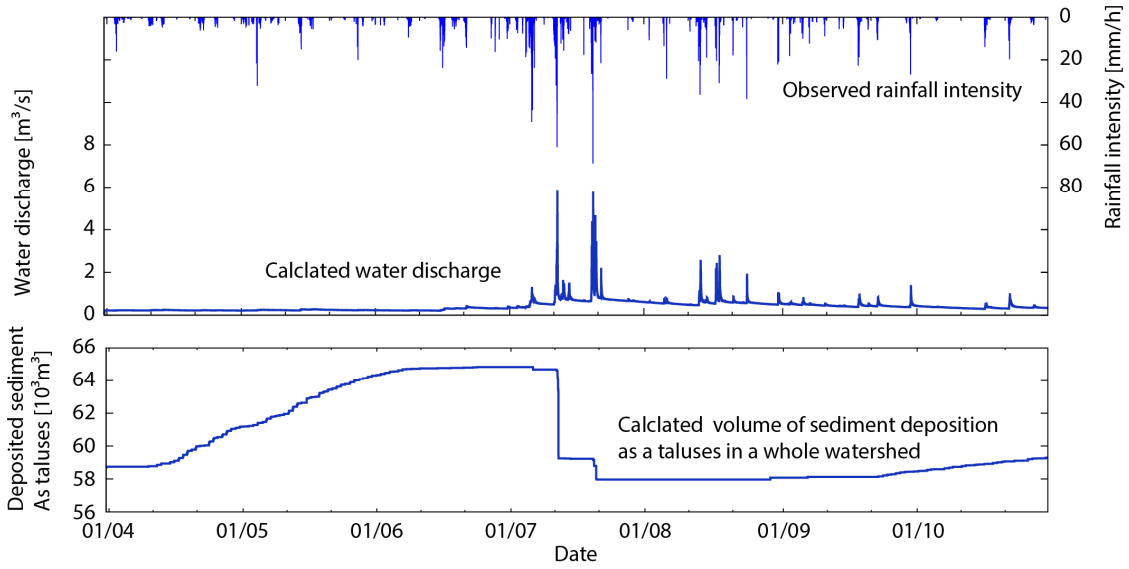

Fig. 7 Observed rainfall intensity and calculated water discharge at the downstream end (2012) and calculated volume of sediment deposition as taluses in the entire watershed

3.2 Results and discussion

In this section, results of calculations were delivered using alternative viewpoints, such as the temporal and spatial variation of deposited sediment, grain size distribution on an annual scale, and the change in relationship between water discharge and sediment discharge. These viewpoints were used to validate the performance and advantages of the model.

3.2.1 Sediment routing in a mountainous watershed

Firstly, observed rainfall intensity and calculated water discharge at the downstream end (in 2012) are shown in **Fig. 7**. Several floods occurred from July to August of this year, and the two floods on July 12 and 20 were the largest. The total volume of sediment deposition as taluses in the basin was also described in the lower part of the Figure. The decrease in sediment deposition implied that sediment supply occurred at the time. Because the sediment was mainly produced from April–May by freeze-thaw action when the air temperature fluctuated between plus and minus Celsius, the deposition volume was thus increased during the period. In relation to the two largest floods, the volume of sediment deposited as taluses decreased in stages, which implied that sediment supply occurred at these times. From the end of September, the volume of sediment began to increase again in relation to the freeze-thaw action during autumn. This routing seemed to be typical sediment production and supply processes in Japanese mountainous watersheds.

In this model, sediment deposition was described by the two morphologies (e.g. talus sediment and riverbed aggradation). The spatial variation of these morphologies appeared to be important in synthetic sediment management because the information gained was directly linked to sediment runoff rates in a mountainous watershed. The variation in time series of the volume of sediment deposited as taluses at the toe of slopes is described using a color variation for each slope in **Fig. 8**. The deposition depth of the sediment, which was determined by the change in riverbed elevation from the initiation of calculations, was also shown by the thickness of the lines within the Figure.

On 01/04 (when the calculation began), there were no fresh sediment deposits on either taluses or on the riverbed. After sediment production during the spring until June, a large amount of sediment was deposited at the toe of slopes as taluses. However, until this point there appeared to have been almost no sediment supply, because no large floods had occurred prior to the July floods.

On 24/07, sediment deposition appeared on the riverbed (particularly in the upstream end) from sediment supply in relation to the two largest floods occurring during the year. Most of the river bed sediment deposition was located near sediment sources during this period. However, this was then flushed out by following flooding. After all the floods in the year had passed, a certain amount of supplied sediment remained, and on 30/11, this was found to be distributed rather evenly. During this period, the amount of sediment deposited as taluses increased again in relation to sediment production from the freeze-thaw action during the autumn season. In this model, we were able to qualitatively simulate this sediment routing process in a mountainous watershed.

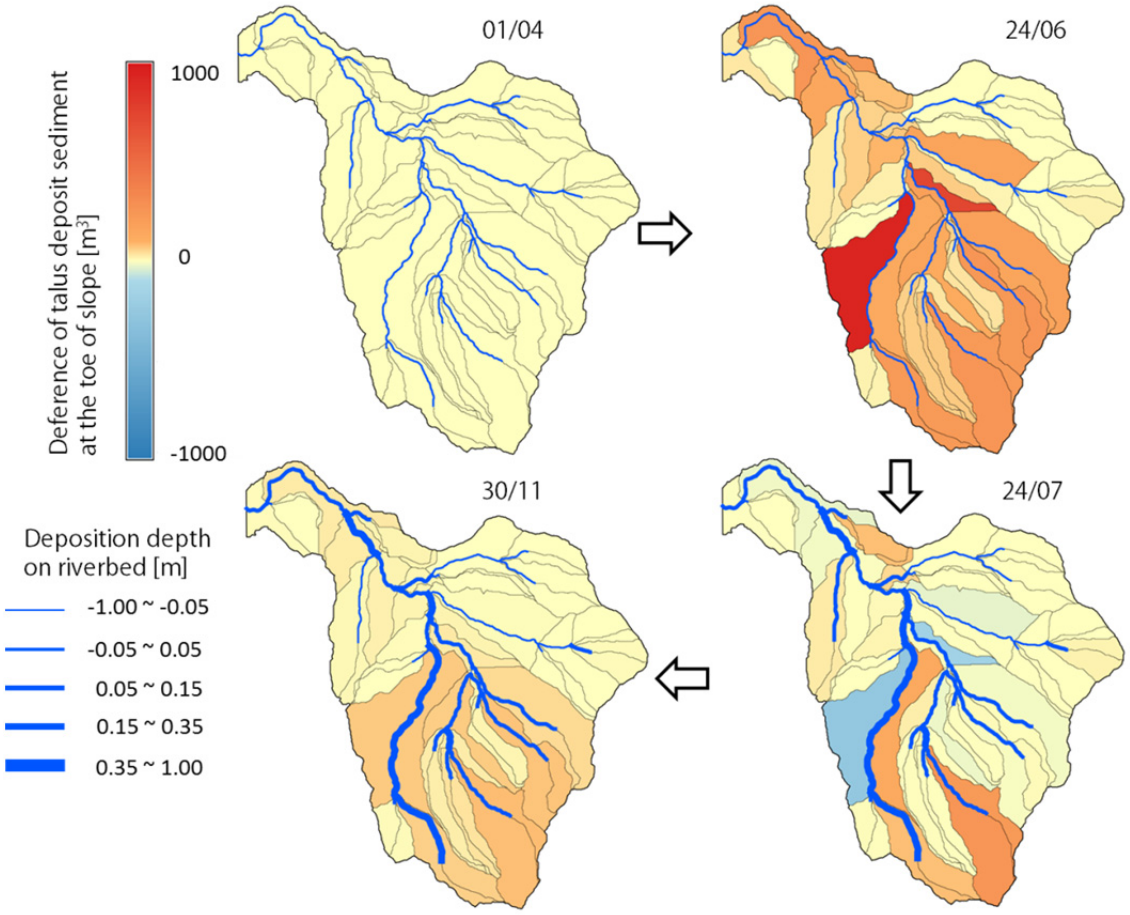

Fig. 8 Amount of talus sediment and deposition depth on the riverbed on four different dates

3.2.2 Differences in grain size distribution between upstream and downstream

In this type of sediment runoff routing, the grain size distribution of bed material also changed with the sediment supply, because the grain size of supplied sediment was finer than the river bed material. **Fig. 9** shows the changes in the mean diameter of exchange layer during the flood season in July at three different points (shown as points U, M, and D in **Fig. 4**). The mean diameter at point U in the upstream reach fell suddenly after the supply of sediment, and immediately rose again in relation to the relatively large volume of supplied sediment transported by the high tractive force during the flood. In other words, the change in mean diameter depended here not on the transported sediment from upstream, but on the sediment supply. In contrast, the change in mean diameter at the downstream reach (Point D) did not quickly rise immediately after falling. This meant that the main reason for a decrease in mean diameter was related to the transported sediment from upstream, and the influence from sediment supply was relatively low. At the middle reach (Point M), the change in mean diameter displayed complex changes. This indicated that the mean diameter of the riverbed material here was influenced by both sediment transport from upstream and sediment supply. In conclusion, our calculation results showed that the characteristics in mean diameter change differed depending on the location of the sediment within the watershed. This temporal change in grain size distribution made a relation between sediment discharge and water discharge variable, which implied a specific characteristic of sediment runoff in mountainous watersheds.

3.2.3 Comparison of sediment runoff characteristics

When the sediment is supplied or transported, the characteristics **of** sediment runoff could be changed according to the change of mean diameter of riverbed material. **Fig. 10** shows a comparison of the relationship between deposited sediment, water discharge, and sediment discharge at points U, M, and M2 shown in **Fig. 4**. In the upper part of each of the three graphs, the volume of deposited sediment was seen as taluses. In the spring season, sediment production occurred with a different intensity, but this period occurred late at point U because of the high elevation. At this point, sediment supply

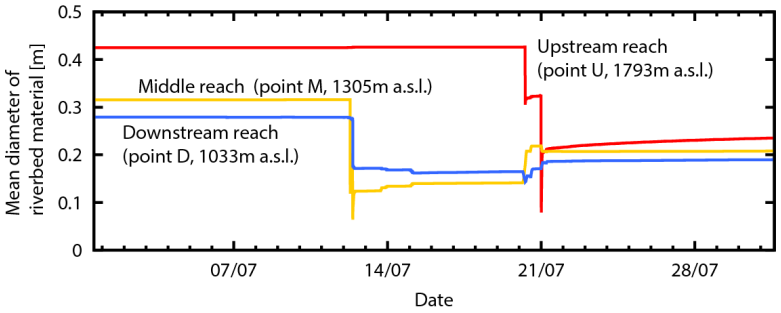

Fig. 9 Change of mean diameter of exchange layer during the flood season

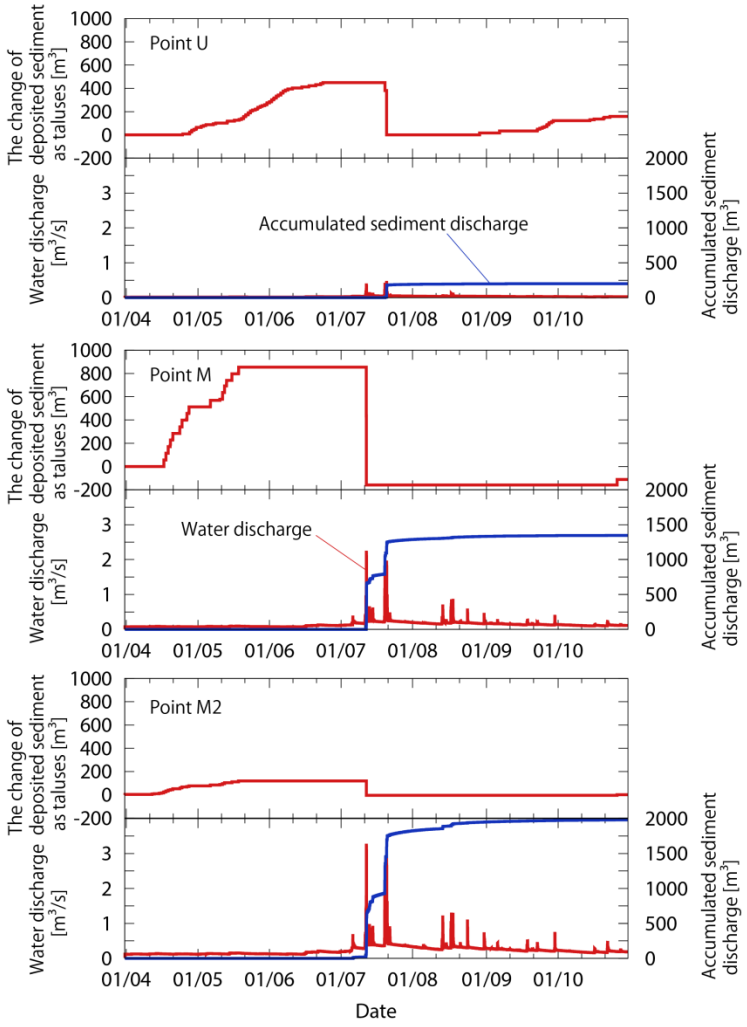

Fig. 10 Comparison of the relation between deposited sediment, water discharge, and sediment discharge

happened only by a flood of July 20 (the second large flood). As a result, there was no sediment runoff during the flood of July 12 (the first large flood) despite the fact that the flood scale was almost the same.

At point M, the amount of sediment supply on July 12 was large enough to enable sediment runoff. The scales of both sediment runoff events were large and almost the same. However, almost no sediment runoff occurred after August in this year, which indicates that large part of the sediment had already run off and the mean diameter of the sediment rather increased by the end of July.

In contrast, sediment runoff occurred twice on a large scale at point M2, despite the low rate of sediment supply, because sediment was transported from point M. Additionally, sediment runoff occurred not only during the two large floods, but also in August. This was probably attributed to the fact that a certain amount of sediment remained on the river bed at point M2 just after the second large flood. The delay in sediment transport between M and M2 was therefore adequately expressed using this integrated model.

4. CONCLUSIONS

In this paper, we applied the integrated sediment runoff model to a small watershed and discussed the sediment runoff process computed by the integrated model. As a result, the sediment runoff process in a mountainous watershed was simulated in detail. Sediment was initially produced by weathering due to freeze-thaw action, and it then formed taluses at the bottom of the valley. Secondly, the taluses were eroded by stream flow that occurred mainly during the two floods in July, which enabled sediment to be supplied to the stream channel. Thereafter, the sediment was transported downstream. The spatial variation in sediment deposition as taluses or on the riverbed was simulated and visualized in the model using GIS processing. At times, the sediment supply caused a reduction in the mean diameter of riverbed material, which subsequently increased in the upstream reach, although the mean diameter variation in the downstream reach appears to be dependent on sediment transport from upstream. In relation to these influences, the relationship between water discharge and sediment discharge changed widely. The transition of the relationship was described by comparing the volume of sediment deposited as taluses. Results showed that the relationship was influenced by the amount and timing of sediment supply, the spatial distribution of sediment sources, and the temporal variation in the volume of sediment deposited. These results implied that the integrated model could provide a greater amount of detailed sediment runoff process information in comparison with previous sediment runoff models that were based on statistical methods, and it could therefore contribute to advancements in synthetic sediment management.

REFERENCES

Ashida, K., Takahashi, T. and Sawada, T. (1983) Runoff process, sediment yield and transport in a mountain watershed (12), Annuals of Disaster Prevention Research Institute, Kyoto Univ., 26B-2, 303–314 (in Japanese with English abstract)

B. Y. Liu (1991) Study on Sediment Transport and Bed Evolution in Compound Channels, PhD Thesis, Kyoto University, Japan

Egashira, S. and Matsuki, T. (2000) A method of predicting sediment runoff caused by erosion of stream channel bed, Annual Journal of Hydraulics Engineering, Japan Society of Civil Engineers, Vol. 44, 735–740 (in Japanese with English abstract)

Fujita, M., Sawada, T, Shida, M. and Itoh, M. (2005) Characteristics on sediment production in the Takahara River Basin, Annual Journal of Hydraulics Engineering, Japan Society of Civil Engineers, Vol. 49, 1075–1081 (in Japanese with English abstract)

Fujita, M., Yamanoi, K. and Izumiyama, H. (2014) A Combined Model of Sediment Production, Supply and Transport, Sediment Dynamics: From the Summit to the Sea, ICCE/IAHS International Symposium (Accepted)

Izumiyama, H., Tsutsumi, D. and Fujita, M. (2012) Effect of freeze-thaw action on porosity change and destruction of weathered bedrock in different lithology and development of destruction model, International Journal of Japan Erosion Control Engineering, Vol. 5, No.1, 103–112

Matsuoka, N. (1990) The rate of bedrock weathering by frost action, Earth Surface Processes and Landforms, Vol. 15, 73–90

Mouri, S., Hayashi, S., Kameyama, S. and Watanabe M. (2001) Fundamental study on modelling of sediment routing through forest and agricultural area in watershed, Annual Journal of Hydraulics Engineering, Japan Society of Civil Engineers, Vol. 45, 799-804 (in Japanese with English abstract)

Murakami, G., Shiiba, M., Hori, T. and Ichikawa, Y. (2003) Modeling of water and sediment dynamic in the basin scale and its application to the actual basin, Annual Journal of Hydraulics Engineering, Japan Society of Civil Engineers, Vol. 47, 733-738 (in Japanese with English abstract)

Sawada, T., Ashida, K. and Takahashi, T. (1982) Variation on stream channel and sediment transport in mountain region, Proceedings of the Japanese Conference on Hydraulics, Vol. 26, 105-110 (in Japanese)

Sunada, K. and Hasegawa, N. (1994) Study on a synthetic model for sediment routing in a mountainous river system, Journal of the Japan Society of Civil Engineers, No. 485/II-26, 37–44 (in Japanese with English abstract)

Takahashi, T., Inoue, M., Nakagawa, H. and Satofuka, Y. (2000) Prediction of sediment runoff from a mountain watershed, Annual Journal of Hydraulics Engineering, Japan Society of Civil Engineers, Vol. 44, 717–723 (in Japanese with English abstract)

Tsutsumi, D., Fujita, M., Itoh, M., Teshima, H., Sawada, T., Kosugi, K. and Mizuyama, T. (2007) Fundamental study on sediment yield due to freeze and thaw process, Journal of the Japan Society of Erosion Control Engineering, Vol. 59, No. 6, 3–13 (in Japanese with English abstract)

Yamanoi, K. and Fujita, M., (2014) Development of a combined model of sediment production, supply and transport and its application to a mountainous basin, Journal of the Japan Society of Civil Engineers B1, Vol. 70, I_925–I_930 (in Japanese with English abstract)

Wegmann, M., Gudmundsson, G.H. and Haeberli, W. (1998) Permafrost changes in rock wall and the retreat of alpine glaciers, Permafrost and Periglacial Processes, Vol. 9, 23–33